Revisit laser scanning fluorescence microscopy performance under fluorescence-lifetime-limited regime

Antony C. Chan, Terence T. W. Wong, Kenneth K. Y. Wong, Edmund Y. Lam, Kevin K. Tsia

Antony C. Chan, Terence T. W. Wong, Kenneth K. Y. Wong, Edmund Y. Lam, Kevin K. Tsia, "Revisit laser scanning fluorescence microscopy performance under fluorescence-lifetime-limited regime," Proc. SPIE 8947, Imaging, Manipulation, and Analysis of Biomolecules, Cells, and Tissues XII, 894726 (4 March 2014); doi: 10.1117/12.2038766

SPIE.

Event: SPIE BiOS, 2014, San Francisco, California, United States

Revisit Laser Scanning Fluorescence Microscopy Performance under Fluorescence-lifetime-limited Regime

Antony C. Chan[a], Terence T. W. Wong[a], Kenneth K. Y. Wong[a], Edmund Y. Lam[a] and Kevin K. Tsia[a]

[a]Department of Electrical and Electronic Engineering, The University of Hong Kong, Hong Kong, China.

ABSTRACT

Continuing desire for higher-speed laser scanning fluorescence microscopy (LSFM) and progressive advancement in ultrafast and sensitive photodetectors might imply that our conventional understanding of LSFM is not adequate when approaching to the intrinsic speed limit — fluorescence lifetime. In this regard, we here revisit the theoretical framework of LSFM and evaluate its general performance in lifetime-limited and noise-limited regimes. Our model suggests that there still exists an order-of-magnitude gap between the current LSFM speed and the intrinsic limit. An imaging frame rate of $> 100\,\mathrm{kHz}$ could be viable with the emerging laser-scanning techniques using ultrafast wavelength-swept sources, or optical time-stretch.

Keywords: laser scanning fluorescence microscopy, image resolution, signal-to-noise ratio, speed limit

1. INTRODUCTION

Fluorescence microscopy provides superior image contrast against unlabelled background, thanks to the high staining specificity of fluorophores to the targeted specimen. The introduction of laser as a coherent excitation source further improves image quality, by providing efficient fluorophore excitation, including multi-photon fluorescence excitation, and localized excitation area. Therefore, the laser-scanning fluorescence microscopy (LSFM) is nowadays welcomed among biomedical researchers who apply this technology to reveal detail biomolecular events with high contrast and high resolution.[1]

Nevertheless, LSFM cannot compete with wide-field microscopy in terms of imaging temporal resolution. To construct a two dimensional image, the excitation spot must be scanned along both x,y-axes. The effective imaging frame-rate is thus limited by the time it requires to complete one scanning cycle. It explains that LSFM has seldom been utilized for studying fast dynamical biological events, such as neuronal action potentials, cellular chemical waves and drug transport.[2–4]

Attempts have been made to improve the scanning speed in LSFM by reducing the inertia of moving components, or even eliminating them. Light-weight mechanically scanning mirrors is now widely adopted in commercial laser scanning microscopes, having an one-dimensional (1D) scan rate from $\sim 0.1\,\mathrm{Hz}$ frame rate to $\sim 1\,\mathrm{kHz}$.[5] By driving the mirrors at their resonant frequencies, the scanning speed can reach up to $\sim 10\,\mathrm{kHz}$.[5] The inertia of the moving components is further reduced with an acousto-optic deflector (AOD), in which the laser is deflected by the frequency-dependent acoustic wave driven by a piezoelectric transducer,[1,6] thus pushing the scan rate up to $\sim 10 - 100\,\mathrm{kHz}$.[7] An emerging laser-scanning technique involves wavelength-to-space encoding utilizing a wavelength-swept laser source and a diffraction grating, demonstrating a scan rate of $40\,\mathrm{kHz}$ on non-biological samples.[8] Notably, all mechanical components of the wavelength-swept laser source can be eliminated by optical time-stretch process,[9–12] thus can drastically scale up the scan rate to $\sim 100\,\mathrm{MHz}$.

While laser scanning technology is continually evolving and progressively higher scanning speed is realized, the scanning speed is intrinsically limited by the fluorescence lifetime, which is in the order of $\mathrm{ns}-\mu\mathrm{s}$.[13] When the

Further author information: (Send correspondence to Kevin K. Tsia)
Antony C. Chan: E-mail: cschan@eee.hku.hk
Kevin K. Tsia: E-mail: tsia@hku.hk

Imaging, Manipulation, and Analysis of Biomolecules, Cells, and Tissues XII, edited by Daniel L. Farkas, Dan V. Nicolau, Robert C. Leif, Proc. of SPIE Vol. 8947, 894726
 · doi: 10.1117/12.2038766

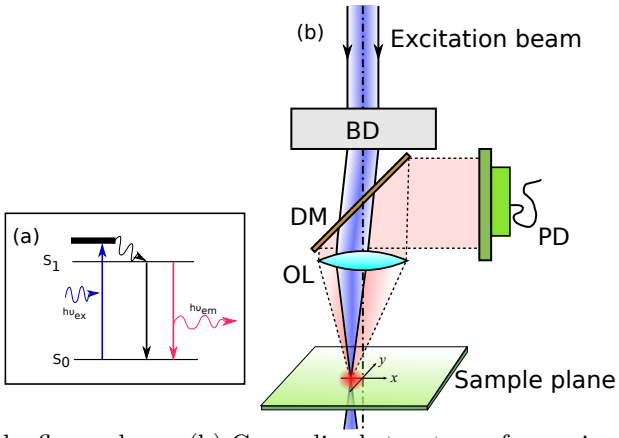

Figure 1: (a) Energy states of the fluorophore. (b) Generalized structure of scanning microscopy for fluorescence sample. (Key: *BD*: beam deflector; *OL*: objective lens; *DM*: dichroic mirror; *PD*: photodiode.)

scanning dwell time approaches to this time scale, fluorescence decay degrades image quality. Hence, diffraction-limited resolution[1,14–17] alone is inadequate to evaluate system performance at high speed. In this paper, we present an improved model which takes into account of fluorescence dynamics into spatial resolution evaluation. We also evaluate the impact of photon noise to the image quality. The analysis allows us to understand how far we can boost the scanning speed without degrading resolution, either in the *lifetime-limited* or *noise-limited* regime. Our numerical results also predicts that an LSFM at 1D scan rate of $> 100\,\mathrm{kHz}$ can be achieved without significantly degrades resolution. We anticipate that this study can provide new insight of developing ultrafast LSFM which could benefit high-speed imaging the dynamical processes of biological systems as well as high-throughput screening applications.

2. TRADITIONAL MODEL OF LASER SCANNING FLUORESCENCE MICROSCOPY

Traditional laser scanning fluorescence microscopy assumes that fluorescence emission intensity on the sample plane follows the excitation field during scanning. For a laterally scanning excitation source, approximated as a Gaussian beam, the emission intensity is given by

$$\varphi_{\mathrm{em}}(x;t) = \varphi_{\mathrm{ex}}(x;t) = \exp\left[-\frac{1}{2}\left(\frac{x-vt}{w}\right)^2\right], \tag{1}$$

where w is the beam waist of the Gaussian beam, and v is the scanning speed of the beam at the sample plane. For the sake of argument, a number of proportionality constants, such as optical power and photon energy, are omitted in this section.

The emission photons are collected back by the objective and relay lens system (Figure 1b). The combined diffraction effect degrades the emission field when it strikes on the plane of the photodetector. Let $h(x)$ be the *point spread function* (PSF) of the optical system, and $\varphi_{\mathrm{em}}(x;t)$ be the fluorescence emission distribution on the sample, the optical intensity that strikes the plane of photodetector is the convolution of both terms, i.e. $|h(x)|^2 * \varphi_{\mathrm{em}}(x;t)$. The single-pixel photodetector then sums up all fluorescence emission to produce a photocurrent

$$i(t) = \int_{-R}^{+R} |h(x)|^2 * \varphi_{\mathrm{em}}(x;t)\,dx, \tag{2}$$

where R denotes the radius of the finite aperture of the photodetector. Again all proportionality constants including magnification power, objective collection efficiency and quantum efficieny of the fluorophore are omitted from the equation. If the aperture radius is chosen to be much larger than the emission spot ($R \gg w$), the term

$|h(x)|^2$ vanishes, i.e.

$$i(t) = \exp\left[-\frac{1}{2}\left(\frac{x-vt}{w}\right)^2\right]. \tag{3}$$

This expression is essentially the PSF of the laser scanning fluorescence microscopy, as the temporal photocurrent signal can be mapped to corresponding location on the sample at $x_s = vt$. If we apply Fourier transform to Eq. (3), we obtain the *optical transfer function* (OTF) of the system

$$I(k) = \exp\left(-\frac{1}{2}w^2k^2\right), \tag{4}$$

where k denotes the lateral spatial frequency with a unit of $2\pi/w$. The OTF evaluates the image contrast against image background (i.e. average signal level) of a sinusoidal fluorophore pattern on the sample at specific spatial frequency k. If we define Rayleigh resolution as the 25% contrast at cut-off spatial frequency k_{Ray},[1] we have

$$\begin{aligned}\exp\left(-\frac{1}{2}w^2k_{\text{Ray}}^2\right) &= 25\% \\ \Rightarrow k_{\text{Ray}} &= 1.67/w.\end{aligned} \tag{5}$$

This traditional resolution metric is shown as dotted line in Figure 2.

3. CONSIDERATION OF FLUORESCENCE LIFETIME

At ultrahigh scanning speed, the assumption in Eq. (1) no longer holds. To model the temporal interaction of excitation and fluorescence emission, we derive the fluorescence dynamics based on two-state Jablonski diagram (Figure 1a). Let $p_1(x;t)$ be the probability of a fluorophore in the excited state (S_1), the rate equation of S_1 is given by

$$\frac{dp_1(x;t)}{dt} = -\frac{p_1(x;t)}{\tau} + \varphi_{\text{ex}}(x;t) \times [1 - p_1(x;t)] \tag{6}$$

$$\simeq -\frac{p_1(x;t)}{\tau} + \varphi_{\text{ex}}(x;t), \tag{7}$$

where τ is the fluorescence decay lifetime. The linear approximation in Eq. (7) holds true if the fluorophore is not driven to saturation at high excitation power. Solving this differential equation and substituting the expression of φ_{em} back to Eq. (2), we obtain

$$i(t) = \exp\left(-\frac{t}{\tau}\right) * \exp\left[-\frac{1}{2}\left(\frac{x-vt}{w}\right)^2\right]. \tag{8}$$

Again this temporal photocurrent is mapped to corresponding location on the sample x_s. Since the fluorescence decay and its associated emission spatial profile are asymmetric, the corresponding OTF has a phase factor. If we ignore phase response of the system, we obtain *contrast transfer function* (CTF)

$$\left|\frac{I(k)}{I(0)}\right| = \frac{\exp\left(-\frac{1}{2}w^2k^2\right)}{\sqrt{(v\tau)^2k^2+1}}. \tag{9}$$

It can be shown that Eq. (9) approximates to Eq. (4) when scanning speed is much smaller than the critical speed, i.e. $|v| \ll v_c = w/\tau$. For conventional LSFM of beam radius at around 1 μm and typical fluorescence lifetime at around 10 ns, the critical speed $v_c = 100\,\text{ms}^{-1}$. For a full-scanning range of around 100 μm, the critical 1D scan rate is 1,000 kHz. If the scanning speed v is comparable to the critical speed v_c, the Rayleigh resolution is given as

$$\begin{aligned}\frac{\exp\left(-\frac{1}{2}w^2k_{\text{Ray}}^2\right)}{\sqrt{(v\tau)^2k_{\text{Ray}}^2+1}} &= 25\% \\ \Rightarrow k_{\text{Ray}} &= \frac{1}{w}\sqrt{W\left[16 \times v_n^{-2}\exp v_n^{-2}\right] - v_n^{-2}}\end{aligned} \tag{10}$$

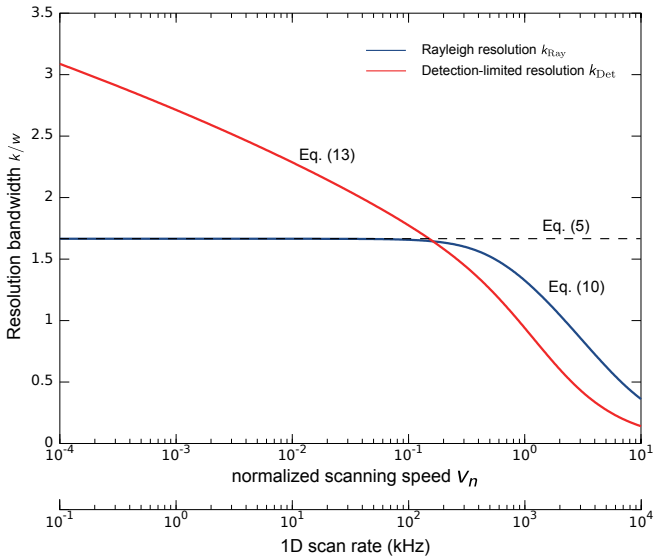

Figure 2: Plot of resolution bandwidth k against normalized scanning speed v_n. The 1D scan rate axis is also added for comparison.

where $v_n = v/v_c = v\tau/w$ is the normalized scanning speed, and $W(z)$ is the Lambert W-Function.[18] Scanning-speed-dependent Rayleigh resolution k_{Ray} is shown as blue line in Figure 2, in which the beam waist $w \simeq 1\,\mu$m, and the fluorescence lifetime $\tau \simeq 10$ ns. It is found that our modified resolution model matches traditional model until it deviates significantly beyond $v_n = 0.1$. Most notably, all the existing scanning technologies, that operate at below 100 kHz 1D scan rate, can be accurately approximated by diffraction-limited model. At 1D scan rate higher than ~ 200 kHz, the Rayleigh resolution degrades exponentially, reaching the value of $k_{\mathrm{Ray}} \simeq 0.4/w$ at 10 MHz. Therefore, optical time-stretch technology in the MHz range may not find a niche in LSFM, unless the full-scanning range is drastically narrowed so that the normalized scanning speed v_n is down-adjusted to around 0.1.

The lifetime dominating effect at high speed is visualized in the left column of Figure 3. The quality of the simulated LSFM image is generally independent of 1D scan rate up to 100 kHz. At ultrahigh scan rate of 10 MHz, the fluorescence decay tail results in smearing effect to the right side of the simulated stained pattern. But the object (line width of $\sim 16\,\mu$m) is still visible at noiseless condition.

4. CONSIDERATION OF PHOTON NOISE

Although we define 25% to be the cutoff contrast, it does not imply features below 25% contrast is *invisible*. In fact, features at low contrast, say at around 24.5%, can be *recovered* by signal processing techniques such as blind deconvolution.[19,20] However, in reality, fluorescence emission signal is corrupted by a number of noise sources, notably the dark current noise, the thermal noise of the photodetector, and the photon shot noise.[1,21] The random fluctuation of photocurrent $\Delta i(t)$ corrupts low contrast signals beyond recovery.[1] Therefore, there is a fundamental contrast cutoff under which the features cannot be recovered by any post-processing techniques, i.e.

$$\frac{\exp\left(-\frac{1}{2}w^2k_{\mathrm{Det}}^2\right)}{\sqrt{(v\tau)^2k_{\mathrm{Det}}^2+1}} = \frac{\Delta i(t)}{\overline{i(t)}}, \tag{11}$$

where $\overline{i(t)}$ is the average photocurrent. Here we denote k_{Det} to be the *detection limited resolution* at shot-noise limited situation.

In this paper, we primarily focus on ultimate shot-noise contribution to LSFM for simplicity. It also sets the lower limit of the noise level for all detector technologies. The signal-to-noise ratio (SNR) is given by

$$\frac{\overline{i(t)}}{\Delta i(t)} = \sqrt{M} = \sqrt{\bar{Q}_{\mathrm{em}}T}, \tag{12}$$

(a) Ground truth

(b) $\leq 100\,\mathrm{kHz}$, noiseless

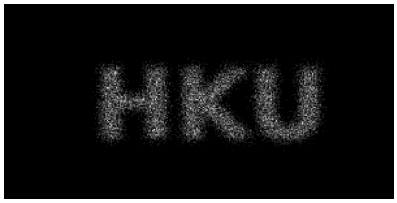

(c) 100 kHz, noise-condition

(d) 10 MHz, noiseless

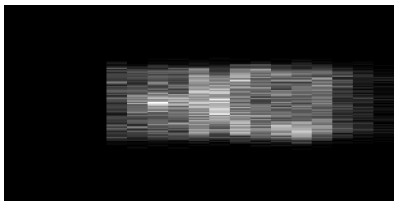

(e) 10 MHz, noise condition

Figure 3: Simulated image of LSFM. The line width of the "HKU" letters are around 16 μm.

where M is the average number of photons received over a sampling interval T. Average emission photon rate $\bar{Q}_{\mathrm{em}}$ consists of the system parameters such as excitation power, absorption efficiency, average concentration of fluorophore, effective emission volume and photon collection efficiency. To maximize SNR, the sampling interval T has to be increased. However, the sampling rate $1/T$ must not be lower than Nyquist sampling limit as it would cause aliasing in the image. Therefore, we set the sampling rate at twice of the detection limit, i.e. $2\pi/(vT) = 2 \times k_{\mathrm{Det}}$. As a result, we obtain an implicit expression of noise-limited resolution k_{Det} of LSFM

$$\frac{\exp\left(-\frac{1}{2}w^2k_{\mathrm{Det}}^2\right)}{\sqrt{(v\tau)^2k_{\mathrm{Det}}^2+1}} = \left[\frac{\pi\bar{Q}_{\mathrm{em}}}{vk_{\mathrm{Det}}}\right]^{-1/2}. \tag{13}$$

The plot of detection-limited resolution k_{Det} in Figure 2 is obtained by assuming emission photon rate $\bar{Q}_{\mathrm{em}} \simeq 10\,\mathrm{photons/\,ns}$. The detection-limited resolution curve is always above the Rayleigh resolution curve up to 1D scan rate of 100 kHz. This may explain why image deconvolution processing is able to recover high-resolution information of images captured from existing scanning technologies. The shrinking gap between the curves predicts the diminishing marginal benefit of contrast-enhancing algorithms. Eventually the crossover takes place at around 200 kHz, which means no more features are visible at the contrast below 25%. Beyond the 1D scan rate of 200 kHz, the cut-off contrast accelerates above 25%. Resolution eventually degrades to $k_{\mathrm{Det}} \simeq 0.15/w$, which is around one-third of Rayleigh resolution k_{Ray} in noiseless case.

The simulated image at shot-noise dominating condition is shown in the right column of Figure 3. Pixelation effect can be seen at 1D scan rate of 100 kHz, as the sampling interval is maximized to optimize SNR. However, the simulated text pattern scanned at 10 MHz is almost unintelligible. It should be noted that the image is not aliased — even if we attempt to capture it at higher sampling rate, no extra information can be extracted as they are all buried under the noise floor. Again, a scan rate 10 MHz may not be an efficient technique for LSFM, unless the fluorescence emission $\bar{Q}_{\mathrm{em}}$ can somehow be raised by boosting the excitation power,[22] improving the photon transfer efficiency,[23] or staining the sample at a higher fluorescence concentration.

5. CONCLUSION

We present a new theoretical model of LSFM which takes into account of the fluorescence dynamics which becomes significant at ultrafast laser scanning speed. The combined effect of diffraction, fluorescence decay and shot-noise enables us to revisit the resolution of existing laser scanning technologies and other emerging ones. It is found that traditional diffraction-limited resolution is an accurate approximation up to 100 kHz. At around 200 kHz and beyond, the resolution degrades exponentially both in the *lifetime-limited* and *noise-limited* regime. Although the ultrahigh scanning technology offered by optical time-stretch may not find a niche in LSFM community, there is still an order-of-magnitude gap between 10 kHz and 100 kHz for existing scanning technology to explore, especially AOD and wavelength-to-space encoding technology. We hope that this theoretical analysis could lay the groundwork for the development of next generation ultrafast LSFM.

ACKNOWLEDGMENTS

The author would like to thank Dr. Ray Xu for discussions and reading the manuscript. This work is partially supported by grants from the Research Grants Council of Hong Kong Special Administrative Region, China (HKU 717510E, HKU 717911E, and HKU 720112E), and the University Development Fund of HKU.

REFERENCES

[1] Pawley, J., "Fundamental limits in confocal microscopy," in [*Handbook of biological confocal microscopy*], 20–42, Springer (2006).

[2] Petty, H. R., "High speed microscopy in biomedical research," *Optics and photonics news* **15**(1), 40–45 (2004).

[3] Kim, K. H., Buehler, C., and So, P. T., "High-speed, two-photon scanning microscope.," *Applied Optics* **38**, 6004–6009 (Oct 1999).

[4] Holekamp, T. F., Turaga, D., and Holy, T. E., "Fast three-dimensional fluorescence imaging of activity in neural populations by objective-coupled planar illumination microscopy," *Neuron* **57**(5), 661 – 672 (2008).

[5] Larson, J. M., Schwartz, S. A., and Davidson, M. W., "Resonant scanning in laser confocal microscopy." http://www.microscopyu.com/articles/confocal/resonantscanning.html (2000).

[6] Xu, J. and Stroud, R., [*Acousto-optic devices: principles, design, and applications*], Wiley New York (1992).

[7] Bansal, V., Patel, S., and Saggau, P., [*A high-speed confocal laser-scanning microscope based on acousto-optic deflectors and a digital micromirror device*], 2124–2127, Institute of Electrical and Electronics Engineers (2003).

[8] Strupler, M., Montigny, E. D., Morneau, D., and Boudoux, C., "Rapid spectrally encoded fluorescence imaging using a wavelength-swept source.," *Optics Letters* **35**, 1737–1739 (Jun 2010).

[9] Goda, K., Tsia, K. K., and Jalali, B., "Serial time-encoded amplified imaging for real-time observation of fast dynamic phenomena.," *Nature* **458**, 1145–1149 (Apr 2009).

[10] Goda, K. and Jalali, B., "Dispersive fourier transformation for fast continuous single-shot measurements," *Nature Photonics* **7**, 102–112 (Jan. 2013).

[11] Wong, T. T., Lau, A. K., Wong, K. K., and Tsia, K. K., "Optical time-stretch confocal microscopy at 1 μm," *Optics Letters* **37**(16), 3330–3332 (2012).

[12] Qiu, Y., Xu, J., Wong, K. K. Y., and Tsia, K. K., "Exploiting few mode-fibers for optical time-stretch confocal microscopy in the short near-infrared window.," *Optics Express* **20**, 24115–24123 (Oct 2012).

[13] Bastiaens, P. I. and Squire, A., "Fluorescence lifetime imaging microscopy: spatial resolution of biochemical processes in the cell.," *Trends in Cell Biology* **9**, 48–52 (Feb 1999).

[14] Waters, J. C., "Accuracy and precision in quantitative fluorescence microscopy.," *Journal of Cell Biology* **185**, 1135–1148 (Jun 2009).

[15] Fujita, K., Kobayashi, M., Kawano, S., Yamanaka, M., and Kawata, S., "High-resolution confocal microscopy by saturated excitation of fluorescence.," *Physical Review Letters* **99**, 228105 (Nov 2007).

[16] Stelzer, E., "Contrast, resolution, pixelation, dynamic range and signal-to-noise ratio: fundamental limits to resolution in fluorescence light microscopy," *Journal of Microscopy* **189**(January), 15–24 (1998).

[17] Nakamura, O. and Kawata, S., "Three-dimensional transfer-function analysis of the tomographic capability of a confocal fluorescence microscope.," *Journal of the Optical Society of America A: Optics, Image Science, and Vision* **7**, 522–526 (Mar 1990).

[18] Weisstein, E. W., "Lambert W-Function." From MathWorld–A Wolfram Web Resource. http://mathworld.wolfram.com/LambertW-Function.html (2014).

[19] Yuan, Y., Papaioannou, T., and Fang, Q., "Single-shot acquisition of time-resolved fluorescence spectra using a multiple delay optical fiber bundle.," *Optics Letters* **33**, 791–793 (Apr 2008).

[20] Leung, R. W. K., Yeh, S.-C. A., and Fang, Q., "Effects of incomplete decay in fluorescence lifetime estimation.," *Biomed Opt Express* **2**, 2517–2531 (Sep 2011).

[21] Petty, H. R., "Fluorescence microscopy: established and emerging methods, experimental strategies, and applications in immunology.," *Microscopy Research and Technique* **70**, 687–709 (Aug 2007).

[22] Cianci, G. C., Wu, J., and Berland, K. M., "Saturation modified point spread functions in two-photon microscopy.," *Microscopy Research and Technique* **64**, 135–141 (Jun 2004).

[23] Zhao, Q., Young, I. T., and de Jong, J. G. S., "Photon budget analysis for fluorescence lifetime imaging microscopy.," *Journal of Biomedical Optics* **16**, 086007 (Aug 2011).